Preprint
UCRL-JC-137721

Molecular Dynamics Simulation of Cascade Damage in Gold

E. Alonso, M. J. Caturla, M. Tang, H. Huang, T. Diaz de la Rubia

This article was submitted to
Materials Research Society Conference, Boston, MA., December 2-5, 1996

February 1, 2000

DISCLAIMER

This work was performed under the auspices of the United States Department of Energy by the University of California, Lawrence Livermore National Laboratory under contract No. W-7405-Eng-48.

Molecular Dynamics Simulation of Cascade Damage in Gold

E. Alonso, M.J. Caturla, M.Tang, H. Huang, and T. Diaz de la Rubia
University of California, Lawrence Livermore National Laboratory, Livermore, CA 94551

Abstract

High-energy cascades have been simulated in gold using molecular dynamics with a modified embedded atom method potential. The results show that both vacancy and interstitial clusters form with high probability as a result of intracascade processes. The formation of clusters has been interpreted in terms of the high pressures generated in the core of the cascade during the early stages. We provide evidence that correlation between interstitial and vacancy clustering exists.

Introduction

The primary damage state in heavy ion, neutron or self- irradiated metals is a result of processes taking place within the lifetime of the displacement cascade. These cascades have been a subject of study for many years, and in particular, molecular dynamics (MD) simulations have been used extensively over the last ten years [1]. From the results of these MD studies, a relatively consistent picture of defect production has developed. Most significant, perhaps, is the fact that these simulations predict that even at low temperature both vacancies and interstitials can be produced either isolated or as defect clusters within the 1 to 100 ps of the cascade lifetime, i.e., without the assistance of significant thermal diffusion. The production of interstitials is due to long replacement collision sequences (RCSs) and other processes that result in clustering and dislocation loop formation directly in the periphery of the cascade. The vacancies appear in the core of the cascade region after resolidification of the melt and depending on the details of the cooling process and the properties of the irradiated material, can also be found in large clusters and Frank dislocation loops. Despite all these efforts however, no clear picture that relates the appearance of interstitial clusters with physical processes occurring within the cascade lifetime has emerged. Moreover, experimental validation of interstitial loop formation in cascades is hampered by the fact that TEM observations are limited by resolution considerations to clusters larger than some 10 Å containing one to several hundred defects and use very thin foils from which small prismatic loops can easily escape. Shimomura et al [2] carried out liquid He irradiations of metals with 14 MeV neutrons and in the thick sections of their samples observed loop growth during annealing below stage III after cold (20K) transfer of the irradiated specimens to the TEM, indicating that interstitial-type dislocation loops were present in the sample after liquid He irradiation.

In this paper, we describe recent MD simulations of cascades in Au using an embedded atom method (EAM) potential for Au [3] that has been modified to account for short

MRS Symp. Proc. V439, p367 (1997)

range interactions during the early stages of the cascade. The results are for 10 and 30 keV cascades and generally show that a large fraction of the produced defects are in clusters. Only in one case, for a 10 keV cascade, did we not find any clustering of the defects. In this case, the defect production efficiency was only about 6% of the NRT standard [4]. Moreover, in no case have we found cascades in which vacancy clustering occurs without interstitial clustering, or viceversa. We discuss the details of the cascade evolution and compare temperature, density and pressure profiles for a case where clusters were found to the case where no clustering took place. We show that the temperature profiles are similar for both cases, but that the hydrostatic and shear pressure profiles are substantially different.

Method

High-energy cascades in the bulk have been generated in gold using MD simulations with the MDCASK code. This code takes advantage of massively parallel computers, and the results were obtained on a 256 node Cray T3D. A fourth-order predictor-corrector algorithm was used to solve the equations of motion. Interatomic interactions were modeled using the EAM potential of Foiles *et al* [3]. The potential was modified by Ghaly et al. [5] to account for short range interaction. Periodic boundary conditions were indeed imposed and a damping function based on the Langevin equation was also included to prevent energy from reentering into the simulation box and to control the temperature. All calculations were performed at constant volume.

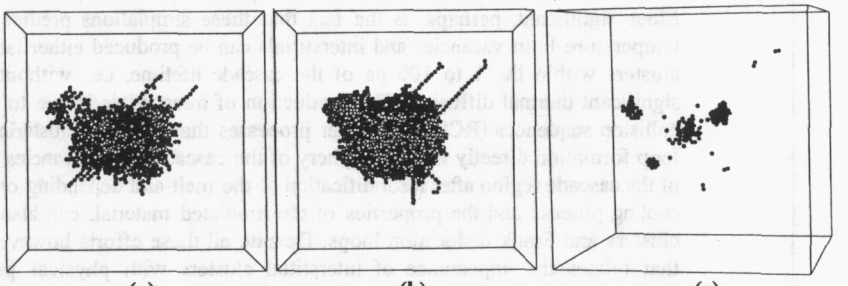

Figure 1. Three snapshots of the displaced atoms during a 10 keV cascade in Au. (a) 0.4 ps, (b) 2.0 ps, and (c) 27 ps. The interstitials (dark circles) are found mostly in clusters, as are the vacancies (light circles)

he results are for 10 and 30 keV
roduced defects are in clusters.
ıny clustering of the defects. In
ıt 6% of the NRT standard [4].
ancy clustering occurs without
s of the cascade evolution and
case where clusters were found
at the temperature profiles are
l shear pressure profiles are

old using MD simulations with
ely parallel computers, and the
ourth-order predictor-corrector
Interatomic interactions were
he potential was modified by
iodic boundary conditions were
evin equation was also included
and to control the temperature.

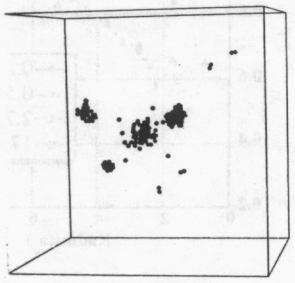

(c)

ı 10 keV cascade in Au. (a) 0.4
s) are found mostly in clusters,

Results and Discussion

Several snapshots of a 10 keV cascade at 50 K are displayed in Figure 1. Notice that the final shape of the cascade is already reached at 0.4 ps. At that point, the onset of the formation of the first cluster is clearly observed, as well as the beginning of the RCSs. The maximum volume of the cascade is reached at about 2 ps. At 27 ps one can consider that the cascade has terminated, this value being the maximum time reached in our MD study. The final number of Frenkel pairs is 66, *i.e.* 66% of the prediction of the NRT collisional model with a 40 eV average threshold displacement energy. More importantly, 62 of them are in clusters. As is expected in metals, the vacancies are distributed in the central core of the cascade while the interstitials are located in the outer part. Most of the vacancies (55) form one big cluster. We also observe a trend in this cluster to evolve to a dislocation loop. This last issue can be checked by extending the simulation time by MD, which would be a tedious task, or coupling MD with force-bias Monte Carlo. The sizes of the interstitial clusters are variable (34, 20, 8). The smallest cluster forms a prismatic dislocation loop and the larger ones exhibit the same tendency as the vacancies. Then, the same procedure could be applied to make sure whether they reach their minimum energy configuration as a loop or not.

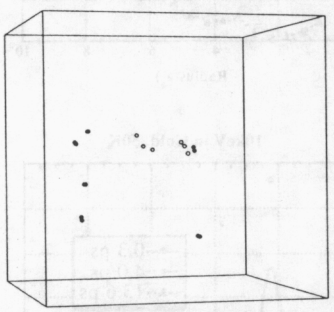

Figure 2. Defect configuration from a 10 keV cascades in Au in which no clusters are formed

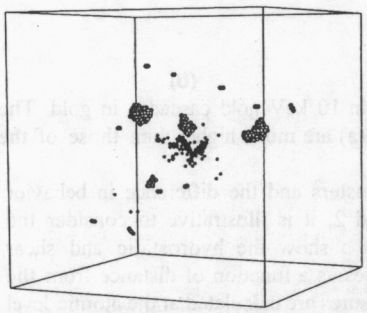

Figure 3. Primary damage state from a 30 keV cascade in Au. The majority of the vacancies and the interstitials are in clusters, as discussed in the text.

Figure 2 shows the final defect configuration generated by another 10 keV cascade at 300 K. In this case, no clusters are observed and the defect production efficiency is only 6% of the NRT prediction. All the interstitials are ejected by RCSs. In figure 3, we show the primary damage state at 60 ps resulting from a 30 keV cascade at 300 K. Here, the defect production efficiency is 30% of NRT (112 Frenkel pairs) and about 70% of the defects are in clusters. About 70 vacancies are clustered in two Frank loops. Only 9 interstitials remain as single type and only 2 as di-interstitials. The rest are present in four clusters of sizes 36, 33, 25 and 7.

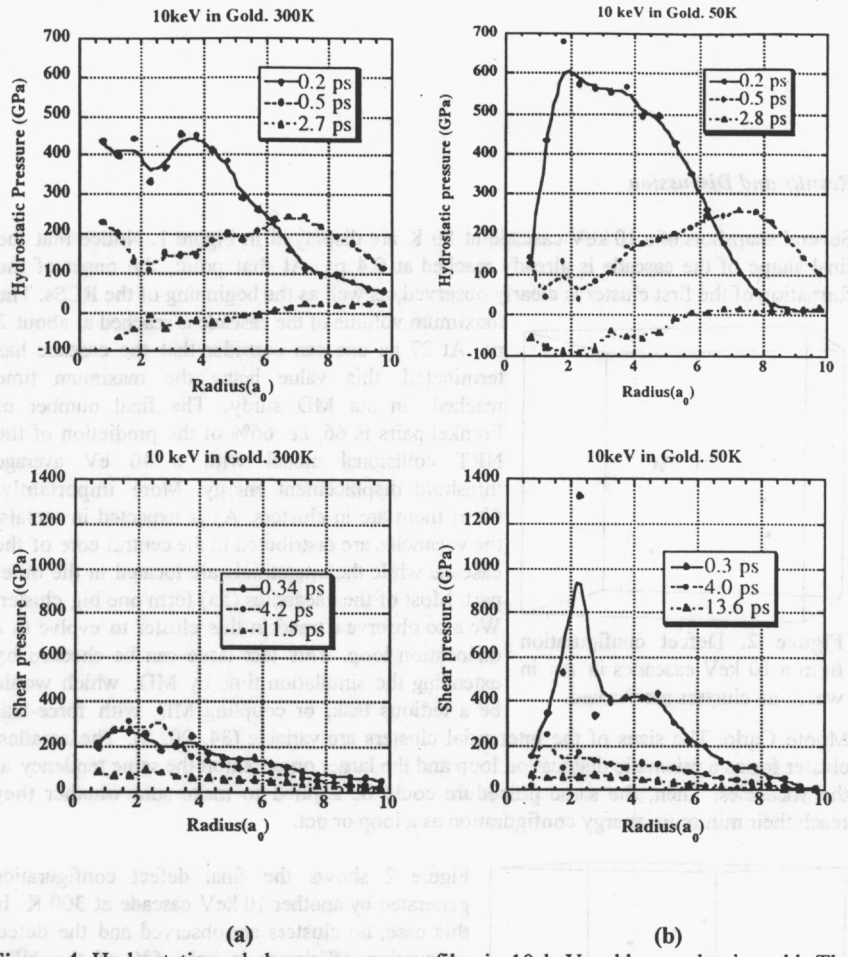

(a) (b)

Figure 4. Hydrostatic and shear pressure profiles in 10 keV gold cascades in gold. The peak values for the cascade with cluster formation (a) are much higher than those of the cascade without clusters (b).

In order to understand the production of defect clusters and the difference in behavior between the two 10 keV cascades of figures 1 and 2, it is illustrative to consider the details of the cascade evolution. Figures 4 a and b show the hydrostatic and shear pressure profiles calculated for both 10 keV cascades as a function of distance from the centroid of energy distribution of each cascade. Pressures are calculated at the atomic level according to the formulation of Vitek *et al* [6]. At short times (around 0.2 ps), when the cluster formation is about to take place, the pressure generated in the first cascade is much higher than in the second one. The extremely large values of the pressures are due to the fact that the calculations are carried out by considering the volume derivatives of the

energy of each atom. Thus, th
times, the region is not yet the
and are in close proximity to
distribution of collision event
establishment of extremely hig
collisions are responsible for sc
clustering. Note also that as sh
the same time as the RCSs. (
cascade region there is a drasti
Figures 5 a and b where radial d
cascade that results in defect clu
than for the cascade that does
significant difference in the tem
any time.

Conclusions

We performed MD simulatio
phenomena. Our results indica
short simulation times (0.2 p
correlation between interstitia

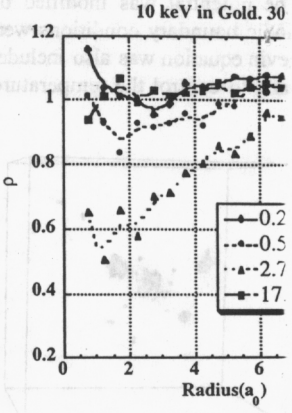

(a)

Figure 5. Radial density profile
is reduced by a factor two in
much higher in the cascade with
small times.

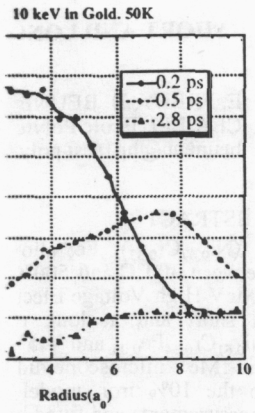

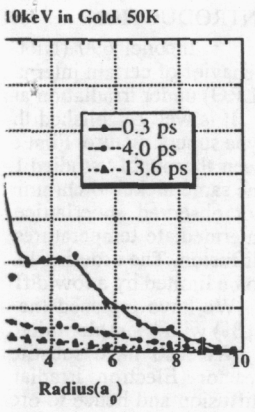

(b)

gold cascades in gold. The
:h higher than those of the

the difference in behavior
llustrative to consider the
he hydrostatic and shear
ction of distance from the
lculated at the atomic level
(around 0.2 ps), when the
in the first cascade is much
.e pressures are due to the
volume derivatives of the

energy of each atom. Thus, the results are skewed by the fact that during these early times, the region is not yet thermalized and many atoms have very high kinetic energies and are in close proximity to other atoms. Nevertheless, the results show that the distribution of collision events during the very early stages of the cascade and the establishment of extremely high pressure gradients as a result of localized high energy collisions are responsible for setting up the conditions for both vacancy and interstitial clustering. Note also that as shown in Fig. 1 the interstitial clusters are ejected at about the same time as the RCSs. Concomitant with the high pressures established in the cascade region there is a drastic reduction in the atomic density. This can be seen in Figures 5 a and b where radial density profiles at various times are shown. Again, for the cascade that results in defect clustering, the density reduction at early times is much larger than for the cascade that does not produce clusters. It is also interesting to note that no significant difference in the temperature profiles for these two cascades were observed at any time.

Conclusions

We performed MD simulations in the bulk and we analyzed interstitial clustering phenomena. Our results indicate that the tremendous increase in pressure occurring at short simulation times (0.2 ps) is responsible for the cluster formation. A strong correlation between interstitial and vacancy clustering can be extracted from our

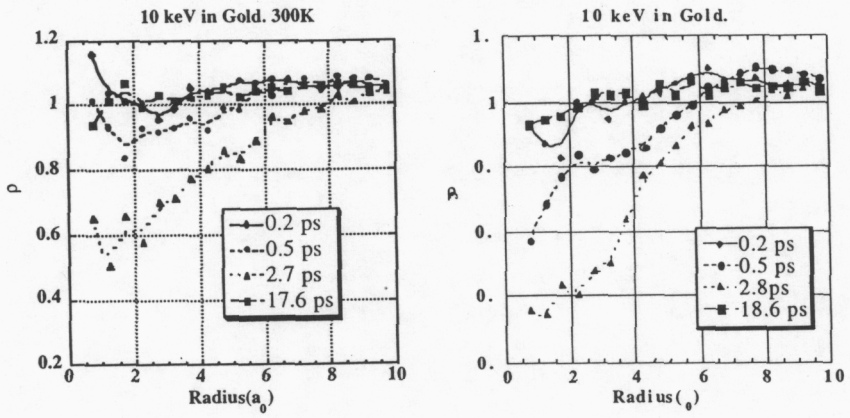

Figure 5. Radial density profiles of 10 keV gold cascades in gold. After 2.7 ps, the density is reduced by a factor two in the cascade without clusters (a). The volume reduction is much higher in the cascade with cluster formation (b) due to the more elevated pressures at small times.

simulations as well as a higher efficiency for cascades where clusters are present. Our results allowed us to extract valuable information on diffusivities to be used in future kinetic-Monte Carlo studies. Ongoing calculations will extend the time scale achieved through MD by using force bias Monte Carlo.

Acknowledgements

This work was performed under the auspices of the US Department of Energy by Lawrence Livermore National Laboratory under contract No. W-7405-Eng-48.

References

1 T. Diaz de la Rubia, *Ann. Rev. Mater. Sci.* **26**, 613 (1996)
2. Y. Shimomura, H. Fukushima, and M.W. Guinan, *J. Nucl. Mater.* **174**, 210 (1990)
3 S.M. Foiles, M.I Baskes and M.S. Daw, *Phys. Rev. B* **33** (1986) 7983-7991
4 M.J. Norgett, M.T. Robinson and I.M. Torrens, *Nuc. Eng. and Design* **33** (1975) 50-54
5. M. Ghaly, Private Communication
6 V. Vitek and T. Egami, *Phys. Stat. Sol. B* **144** (1987) 145-156

SHORT AND LON(

E. FRELY, B. BEUNE
CEA-LSI, Ecole Polyte
beuneub@hp1sesi.poly

ABSTRACT

$(Ni_{0.67}Cr_{0.33})_{1-x}Fe_x$ allo
between 300°C and 500°(
1MeV High Voltage Elect
at short and at long r
$Ni_{0.61}Cr_{0.34}Fe_{0.05}$ and 445°
the 1MeV microscope did
to the 10% iron model
measurements and fitted b

INTRODUCTION

Inconel 690 (Ni6(
behavior of certain interna
(LRO) under irradiation a

It is well established th
type superstructure. First e
been thoroughly studied t
the same nickel to chromi
not observed superlattice
intermediate temperatures
diffusion. The ordering ki
to be limited by a low diff

We have replaced the
at.%) with a simpler micr

We also have substitu
reactor. Electron irradiat
diffusion and hence to orc
is established between def
on sinks (mostly dislocat
magnitude above the therr

The ordering kinetics v

The results of first elec
of all compositions, even

We present here the eff
modelization of data troug

EXPERIMENTAL DETA

Irradiations

Irradiations have been
In our Van de Graaff t

Table I : *typical radiatio*

Electron energy (MeV)
total damage (d.p.a.)
damage rate (d.p.a./s)